Journal of Biomolecular Structure & Dynamics, ISSN 0739-1102
Volume 26, Issue Number 2, (2008)

Structural and Dynamical Studies of Humanin in Water and TFE/Water Mixture: A Molecular Dynamics Simulation

http://www.jbsdonline.com

Faramarz Mehrnejad*
Nader Chaparzadeh

Department of Biology
Faculty of Science
Azarbaijan University of Tarbiat Moallem
Tabriz, Iran

Abstract

The structural and dynamical properties of Humanin, a small peptide with neuroprotective activity against the insults of the Alzheimer's disease-related genes and the neurotoxic amyloid peptide, are studied in two different environments by molecular dynamics simulation. In this study, we have performed comparative molecular dynamics simulations in the absence and in the presence of TFE. The resulting trajectories were analyzed in terms of structural and dynamical properties of peptide and compared to the available NMR data. In water humanin is observed to partly unfold. The peptide is readily stabilized in an ordered helical conformation in the TFE/water mixture. Our simulations show that the peptide is flexible with definite turn point in its structure in water environment. It is free to interact with receptors that mediate its action in polar environment. Humanin may also find an alpha helix structure necessary for passage through biomembranes and/or specific interactions.

Key words: Alzheimer's disease; Molecular Dynamics Simulation; Humanin; Alpha Helix; and GROMACS.

Introduction

2, 2, 2-Trifluoroethanol (TFE) is an important co-solvent in the study of protein and peptide structure. Its effect on the structure of these molecules has been studied for many years and the mechanism by which TFE promotes the stabilization of particular secondary structure elements is beginning to be known (1). The mechanism of peptide stabilization by fluorinated solvents has been investigated by experimental techniques (1) and, more recently, by molecular dynamics simulations (2-5). The results of these investigations have evidenced the presence of a complex mechanism involving a combination of different contributions. In the case of TFE, molecular dynamics simulations show a coating effect of the co-solvent on the simulated peptides, as a possible mechanism of peptide stabilization (2-4). The coating effect is favored by the tendency of the fluorinated solvents to form large clusters in aqueous solution (6, 7). The layer of co-solvent around the peptide reduces the accessibility of the backbone hydrogen bonds to the aqueous solvent, improving secondary structure stability. Among the peptides used to study the effect of fluorinated solvents experimentally, Humanin is one of the most frequently investigated peptides.

Alzheimer's disease is the most prevalent neurodegenerative disease in the ageing population leading to progressive and ultimately fatal loss of mental capacity and it is estimated that 22 million people around the world will be so afflicted by 2025 (8, 9). Humanin is a 24-residue peptide with unique neuroprotective activity against the insults of Alzheimer's disease (10, 11). Humanin was discovered in 2001 (12) by death-trap screening (13) of a cDNA library constructed from the occipital lobe of the brain of an autopsy-diagnosed Alzheimer's disease patient.

*Phone: (+98-412) 4524991
Fax: (+98-412) 4524991
Email: Mehrnejad@azaruniv.edu

This unbiased functional screening of molecules that allow dying cells to survive led to the identification of a cDNA encoding the novel peptide MAPRGFSCLLLLTSEIDLPVKRRA, termed Humanin. The sequence of humanin conforms to the overall structure of signal peptides having a positively charged N-terminal domain, a central hydrophobic region, and a more polar C-terminal domain that terminates with a signal peptidase cleavage site (14, 15). Humanin is secreted from the cells through the endoplasmic reticulum-golgi secretory pathway (11) and acts from the outside of cells potentially through a cell-surface receptor linked to certain tyrosine kinases (16, 17). The potent *in vitro* neuroprotective activity of humanin against the challenged of the Alzheimer's disease-related genes and the neurotoxic beta-amyloid peptide has opened new windows for the development of a pharmaceutical therapy against Alzheimer's disease. To establish therapeutic strategies, as well as to clarify the mechanism of Alzheimer's disease pathogenesis, the mode of humanin action must be understood. Benaki *et al*. showed that in water humanin possessed essentially no stable secondary structure, but interconverted between turn-like conformations in which the regions Gly5-Leu9 and Glu15-Leu18 appeared to be the more ordered (18). This ensemble of secondary structures can be characterized as nascent helix (19) since it is readily stabilized in an ordered helical conformation in the less polar environment of 30% aqueous TFE. The relatively low TFE concentration of 30% required for humanin to acquire its maximum helical content indicates a pronounced helical propensity for the peptide (20). It is thus possible that in the cell, immediately after synthesis, humanin exists predominantly in an unstructured conformation in equilibrium with turn-like structures, but may acquire helical conformation when found in the more lipophilic environment of membranes. The variation in secondary structure of humanin according to the environment may play an important role in the process of its extra cellular secretion. It has been shown (11, 17, 21) that in order to exert cytoprotection, humanin must be secreted into the cultured medium, a fact that indicates that humanin acts only from outside of the cell.

In a recent article, Benaki *et al*., (18) reported an extensive NMR spectroscopic study on the structure of humanin in 30% TFE/water mixture. In the present study, we perform molecular dynamics simulations of humanin in water and in 30% TFE/water mixture in order to investigate at the molecular level the structural and dynamical properties of the peptide in water and TFE/water. The present comparative simulation studies starting from the NMR structures indicate that humanin rapidly unfolds in water in agreement with experiment. In 30% TFE, the helical structure is largely preserved with an average global conformation in good agreement with NMR data. However, the partial unfolding of the helices is seen toward the end of the simulation. The analysis of the distribution of TFE molecules around the peptide allows drawing conclusions on the mechanism of structure stabilization by TFE and the mechanism of helix bending and unfolding.

Materials and Methods

MD simulations were carried out by using GROMACS (22, 23) simulation package on an Intel Dual Xeon PC workstation under Fedora 4. The GROMOS96 force field (24) as implemented in the GROMACS was used (22, 23, 25).

Peptide Model and Solvent Models

The starting atomic coordinate of peptides was obtained from Protein Data Bank (18; pdb codes: 1Y32). The peptide was placed in a periodic truncated cubic and then solvated with water, or a mixture of TFE and water large enough to contain 0.8 nm of solvent on all sides. Water was modeled as rigid three-point molecules using the SPC water model (24), respectively. The TFE parameters were taken from TFE model optimized by Fioroni *et al*. (3). Counter ions (Cl^- and Na^+) were added by replacing water molecules at the most positive/negative electrical potential to achieve

a neutral simulation cell. Under GROMACS each peptide was energy – minimized by using a steepest descent algorithm for 100 steps.

MD Simulation Protocol

In all simulations, the temperature and the pressure were kept close to the intended values (300 K and 1 bar) by using the Berendsen algorithm (26) with $\tau_T = 0.1$ and $\tau p = 0.5$ ps, respectively. Bond length was constrained by using the LINCS algorithm (27). Lennard-Jones interactions were calculated with a 0.9/1.4 nm twin-range cutoff. The short-range electrostatic interactions were calculated to 0.8 nm, and Particle Mesh Ewald algorithm was used for the long-range interactions (28). The neighbor list was updated every 10 steps. Each component of the system (*i.e.*, peptide, water, and TFE) was coupled separately to a temperature bath at 300 K by using a Berendsen thermostat algorithm (26), with the coupling constant $\tau_T = 0.1$ ps. The pressure was kept at 1.0 bar by using isotropic pressure coupling (26) with $\tau p = 0.5$. A time step of 2 fs was used for the integration of equation of motion. All atoms were given an initial velocity obtained from a Maxwellian distribution at the desired initial temperature. All of the simulations, starting from average NMR structure, were equilibrated by 100 ps of MD with position restraints on the peptide to allow for the relaxation of the solvent molecules. Other 100 ps runs followed these first equilibration runs without position restraints on the peptide. The production runs at constant temperature and pressure conditions, after equilibration, were 20000 ps long.

Analysis

The analyses were performed on the ensemble of system configurations extracted at 0.5 ps time intervals from the simulations. Least-squares fitting of atomic coordinate for the calculation of structural properties of the peptide such as the atom-positional root-mean-square deviation or difference (RMSD) were based on the backbone atoms (N, Calpha, C) of all residues. The root-mean square fluctuations (RMSF) were calculated for the C alpha atoms. The secondary structure assignment of peptides for the set structures extracted every 100 ps from the simulation trajectories was done according to the DSSP rules proposed by Kabsch and Sander (29). The hydrogen bonds were calculated using a geometric criterion. A hydrogen bond is defined by a minimum donor-hydrogen-acceptor angle of 135º and a maximum hydrogen acceptor distance of 0.25 nm. The concentration (% vol/vol) of TFE molecules around the peptide residues, named local concentration (LTC), was evaluated from the number of solvent and co-solvent molecules present in a shell of 0.6 nm around the peptide residues and considering the average excluded volume of 0.019 and 0.07 liters·mol^{-1} for water and TFE, respectively (4, 5). The local TFE concentration (LTC) was evaluated from the cumulative number of water [$n_w(r)$] and TFE [$n_T(r)$] molecules present within a distance r from the C_{alpha} of the single residues using the following relation:

$$LTC(r) = \frac{V_m^T n(r)}{[V_m^T n(r) + V_m^W nW(r)]} 100 \qquad [1]$$

Results

Figure 1 contains snapshots of humanin at various time points to illustrate the effects of water and TFE/water on the secondary structure of the peptide. In Figure 2 the rms deviation (RMSD) with respect to the initial structure for the peptide in pure water and TFE/water as a function of time is reported. The humanin backbone remained practically unchanged along TFE/water simulation with an RMSD average below 0.4 nm (Fig. 2). This suggests that the peptide NMR structure is largely maintained its native structure in TFE/water, at least on the time scale sampled in these simulations. After 2000 ps in water, the RMSD reached values up to

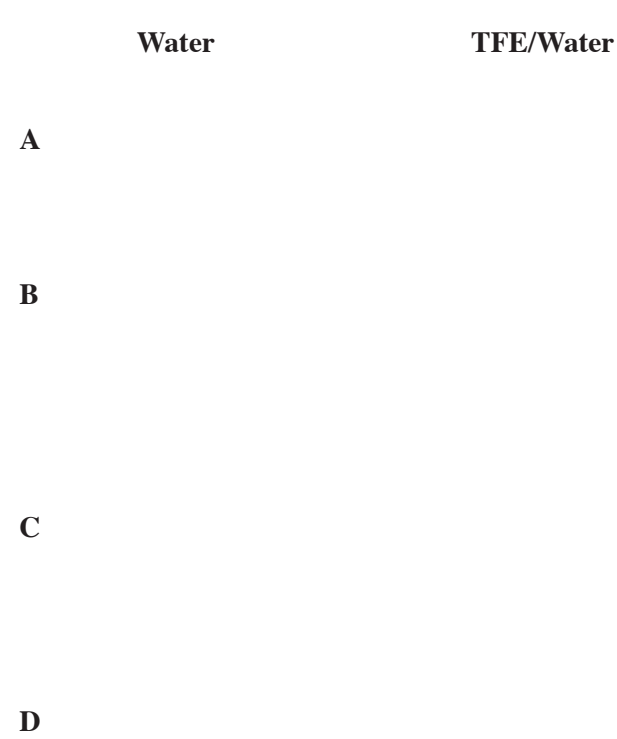

Figure 1: A movie composed of snapshot configurations taken every 7000 ps along picosecond trajectories Humanin in water and TFE/water, respectively.

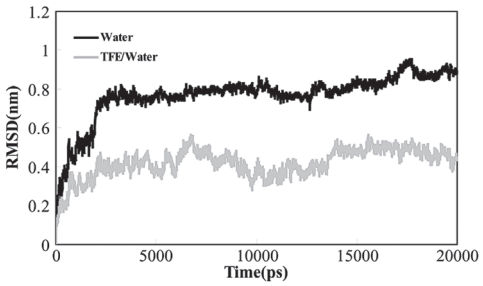

Figure 2: The RMSD of C-alpha atom coordinates of Humanin relative to the starting to the NMR structure, during molecular dynamics simulations in water and TFE/water.

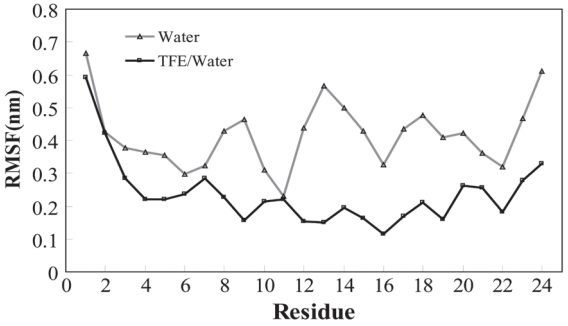

Figure 3: The backbone atomic positional RMSF of Humanin in water and TFE/water.

0.7 nm (Fig. 2). In contrast to its behavior in pure water, in the TFE/water mixture the humanin is stable with the RMSD remaining almost constant at around 0.37 nm for the first 13000 ps of the simulation, rising to 0.4 nm during the last 7000 ps. The atomic positional RMSFs of peptide (Fig. 3) were 0.42 nm in water, 0.23 nm in TFE/water respectively. The RMSF per residue also shows that for humanin the overall mobility of residues in water is larger than that in the TFE/water mixture. The RMSFs confirm the peptide helix is stable in TFE/water environment but less stable in water solution.

The secondary structure of the peptide during the course of the simulations is shown in Figure 4, as defined by dictionary of secondary structure of proteins (DSSP). Comparison of water with TFE/water shows a major difference. For TFE/water the largely alpha helical conformation of the peptide is maintained throughout the 20000 ps duration of the simulation. There are occasional local deviations from alpha helicity in the C-terminal and N-terminal parts of the molecule (Fig. 5). In water, the alpha helicity of peptide decreases at the C-terminus and N-terminus of the molecule starting at 2000 ps and reaching its maximum extent at 15000 ps (Fig. 4).

In Figure 5, the time average of the alpha helicity is reported for the simulations. If we consider as threshold an alpha helicity value of 20%, the helix are comprised between 5-14 for the TFE/water simulation, and 6 and 11 for the water simulation. This is in agreement with the NMR experiments suggesting that the humanin (5-15) region has a potential to adopt an alpha-helical conformation in less polar environments (18). In TFE/water simulation, the original helicity is maintained until 18, while in water simulation, the helix ends after residue 11.

To characterize the conformational variability in the peptide structure, a clustering analysis was performed on simulations. The cumulative number of clusters for water and TFE/water simulations has been plotted as

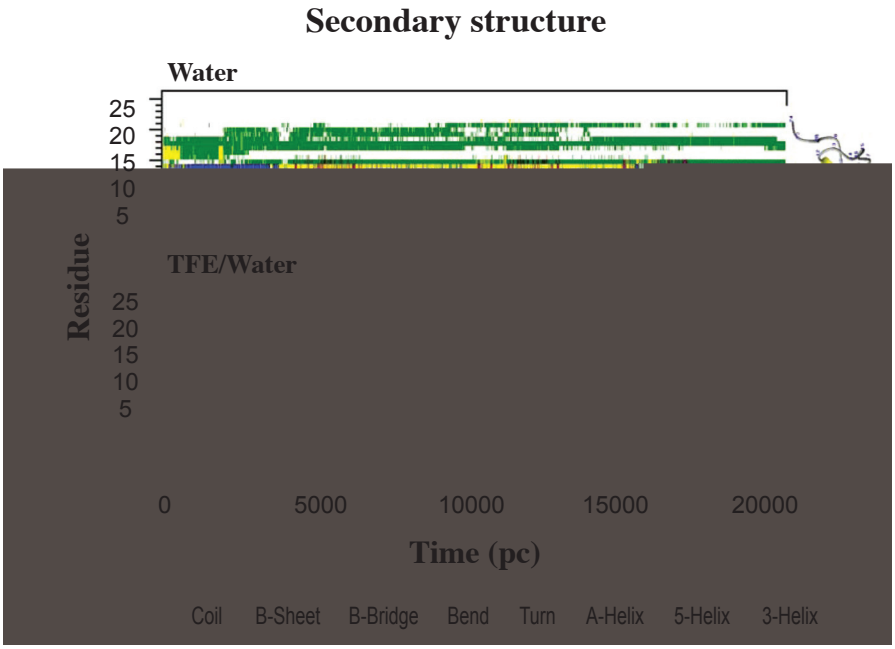

Figure 4: Summery of the secondary structure identified (according to the Kabsch and Sander procedure) in the water and TFE/water simulations.

a function of time (Fig. 6). It is evident that the number of clusters varies between two simulations. In the TFE/water simulation, the number of clusters is less than of that present in water simulation. The larger number of clusters in the water simulation indicates the presence of an enhanced flexibility compared with the simulation in the presence of a 30% TFE mixture.

The analysis of the intramolecular backbone hydrogen bonds basically reflects the observations made in the conformational analysis of the simulations (Fig. 7). Hydrogen bonds characteristic for the alpha helical conformation are largely populated in TFE/water simulation, while in water residues Leu^{10}-Phe^{6}, Leu^{11}-Ser^{7}, Leu^{12}-Cys^{8}, Ser^{14}-Leu^{9} show more than 50% hydrogen bond populations. Sequential loss of the stable hydrogen bonding for residues Leu^{9}-Gly^{5}, Ser^{14}-Leu^{10}, Glu^{15}-Leu^{11}, Ile^{16}-Leu^{12}, Asp^{17}-Leu^{12}, Leu^{18}-Thr^{13}, Val^{20}-Ile^{16}, Val^{20}-Asp^{17}, and Lys^{21}-Pro^{19} occurs throughout the simulation in the water simulation (Fig. 7). The most C-terminus alpha helical hydrogen bond practically disappeared. Unwinding started from C-terminus and propagated toward the N-terminus. In water, the peptide backbone very quickly lost its alpha helical hydrogen bonds beginning from its C-terminus and propagating toward the N-terminus. The 13 initial alpha helical hydrogen bonds formed by humanin were maintained during the entire simulations in TFE/water, while there were not maintained during the water simulation (Fig. 7). In the water simulation, the most alpha helical hydrogen bonds disappeared completely after 500 ps of simulation. In TFE/water, the final structure contained all 13 intra backbone hydrogen bonds. In water simulation, the peptide rapidly lost its initial alpha helical hydrogen bonds. Figure 8 shows the total number of hydrogen bonds between the peptide and solvents over the course of the simulations. In TFE/water simulation, the total number of hydrogen bonds between peptide and TFE increases with time and the total number of hydrogen bonds between peptide and water decreases. The simulation shows that the organic co-solvent accumulates around the peptide forming a matrix that partly excludes water. By accumulating around the solute the TFE molecules exclude water, favoring the formation of intramolecular hydrogen bonds and promoting the formation of secondary structure.

Solvent-induced Conformational Properties

At the beginning of all simulations, the backbone amide hydrogens involved in alpha helical hydrogen bonds were accessible to solvents. Once the simulations proceeded and the alpha helical hydrogen bonds were disrupted, solvent penetra-

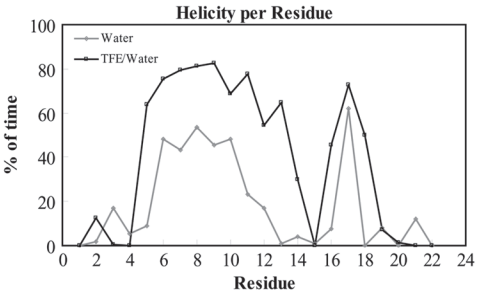

Figure 5: The helicity per residue of Humanin in water and TFE/water simulations.

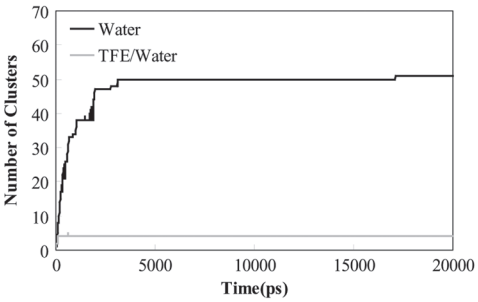

Figure 6: Time course of the different clusters of structures obtained water and TFE/water simulations.

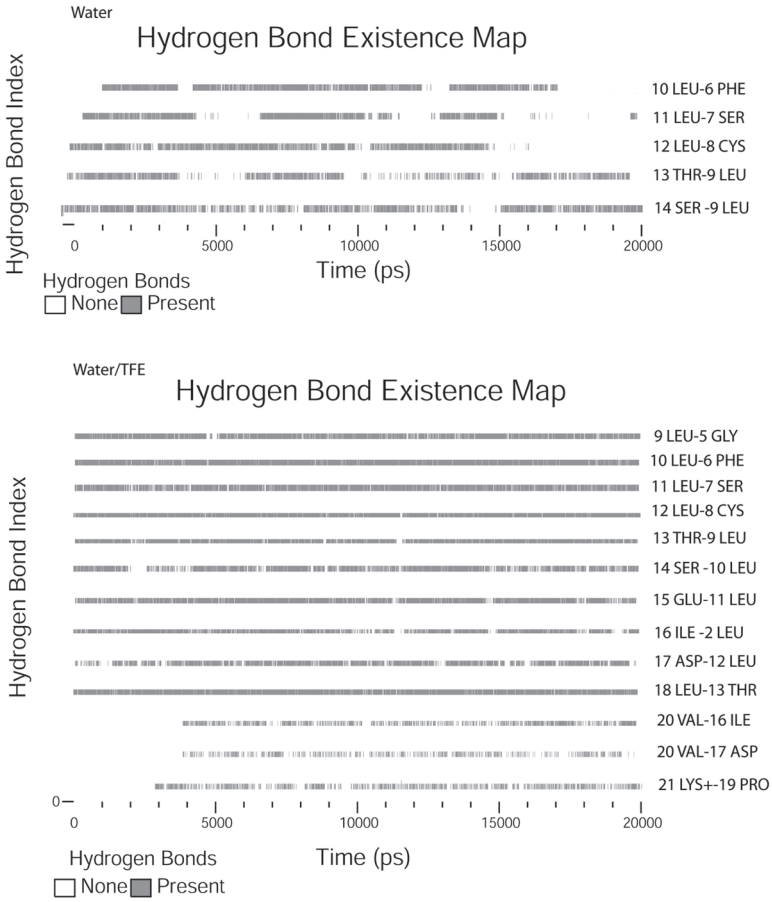

Figure 7: Hydrogen bond existence map for 13 bonds in simulations.

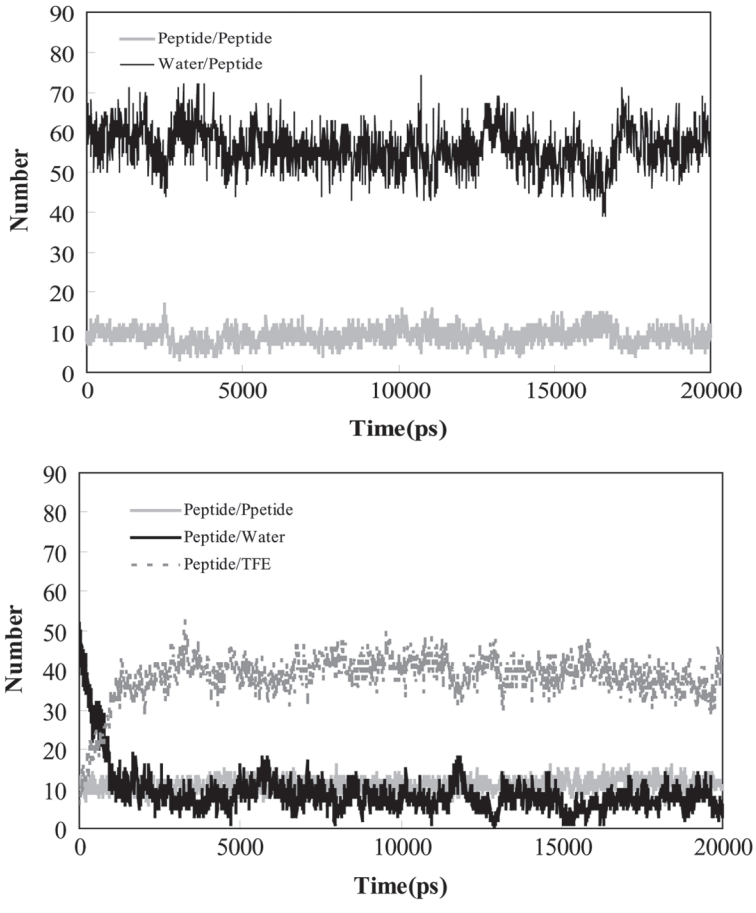

Figure 8: The total number of hydrogen bonds between the peptide-peptide, peptide-TFE, and peptide-water.

tion was observed. In general, the backbone amide hydrogens closest to both ends of the initial alpha helices were more prone to bind solvent. On the contrary, in all simulations, most of the carbonyl oxygens were accessible to solvent and most of the time had solvents molecules attached to them.

In Figure 9, the LTC (local TFE concentration) per residue in the system is reported. The LTC was calculated by determining the relative numbers of TFE and water molecules within a 0.6 nm shell surrounding each residue. In TFE/water the concentration of TFE in close proximity to the helix is on average 2.5 times higher than the bulk. This indicates a strong tendency of the TFE molecules to coat the peptide. In TFE, the interaction between the co-solvent and the peptide is weak (5). Although a layer is formed over the surface of the peptide, the interactions between the peptide and TFE do not displace the peptide-peptide interactions (Fig. 8). A correlation between the presence of alpha helical structure and the increase of LTC around the peptide is present in the TFE/water simulation. It appears that TFE amplifies the local tendency of the peptide to form a preferred secondary structure. Regions with high tendency to form an alpha helix show enhanced coating that, in turn, stabilizes the helix. The ability of TFE to interact with water molecules suggests that the TFE clusters can pull water from surface of helix. TFE matrix may be important to lower the side chain conformational entropy, which is thought to be a key factor in the stabling of alpha helix (30).

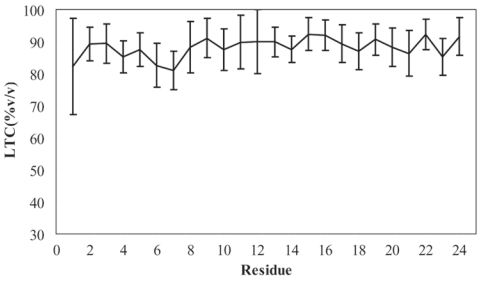

Figure 9: Average local TFE concentration within a distance of 0.6 nm from the C-alpha atom of each residue of Humanin, calculated using the full trajectory of all simulations. Bars indicate the standard deviations.

Discussion

Humanin has neuroprotective activity against the challenged of the Alzheimer's disease-related genes and the neurotoxic amyloid peptide. This potential has offered new methods for the improvement of a pharmaceutical therapy against Alzheimer's disease. To accomplish therapeutic processes, as well as to reveal the mechanism of Alzheimer's disease pathogenesis, the structural and dynamical properties of the peptide in different solvents must be understood.

TFE/water mixtures have been proposed as useful model systems for investigations of the action on peptide structures of the local decrease in dielectric constant like membrane surfaces. The effects of TFE molecules have been referred to lowering the dielectric constant of the solvent, hydrophobic effects, ordering of solvent molecules, changes in hydrogen bonding along the peptide structure, or some combination of these factors (4, 5, 31). Experimental investigation showed that in water Humanin is in an unstructured conformation in equilibrium with turn-like structures involving residues Gly5 to Leu10 and Glu15 to Leu18 and it adopts an alpha helical structure spanning residues Gly5 to Leu18 in the less polar environment of 30% TFE (18).

Molecular dynamics simulations show that in water humanin exists in an unstructured conformation in equilibrium with turn-like structures involving residues Gly5 to Leu10 and Leu12 to Leu18. The peptide is readily stabilized in an ordered helical conformation in the less polar environment of TFE/water mature. At once after synthesis of humanin in the cell, it is in an unstructured conformation in equilibrium with turn-like structures, but may obtain helical conformation when settled in the less polar environment of membranes. The results of simulations evidence a very good correspondence with the experimental NMR data. Furthermore, the simulations show that in a TFE/water mixture the organic co-solvent aggregates around the peptide, forming a matrix that partly excludes water (4, 5). The nonequal distribution of the TFE around the humanin supports the hypothesis of the presence of TFE clusters that interact with the peptide. Therefore, the formation of local interactions are promoted and as a consequence, ordered secondary structure (4). In TFE/water, the interaction between TFE molecules and the peptide residues are weak (32). Although, TFE molecules accumulate around the peptide forming a matrix, the interactions between TFE molecules and peptide do not exchange the peptide-peptide interactions. Our simulations show that the peptide is flexible with definite

turn point in its structure in water environment. It is free to interact with receptors that mediate its action in polar environment. Humanin may also find an alpha helix structure necessary for passage through biomembranes and/or specific interactions.

Acknowledgments

The support of the Azarbaijan University of Tarbiat Moallem is gratefully acknowledged. The invaluable beneficiary of Tarbiat Modares University Molecular Modeling Center is also gratefully acknowledged.

Reference and Footnotes

1. M. Buck. *Q Rev Biophys 31*, 297-355 (1998).
2. M. D. Diaz, M. Fioroni, K. Burger, and S. Berger. *Chem Eur 8*, 1663-1669 (2002).
3. M. Fioroni, M. D. Diaz, K. Burger, and S. Berger. *J Am Chem Soc 124*, 7737-7744 (2002).
4. D. Roccatano, M. Fioroni, M. Zacharias, and G. Colombo. *Protein Sci 14*, 2582-2589 (2005).
5. D. Roccatano, G. Colombo, M. Fioroni, and A. E. Mark. *Proc Natl Acad Sci 99*, 12179-12184 (2002).
6. D. P. Hong, M. Hoshino, R. Kuboi, and Y. J. Goto. *Am Chem Soc 121*, 8427-8433 (1999).
7. K. Gast, A. Siemer, D. Zirwer, and G. Damaschun. *Eur Biophys J 30*, 273-283 (2001).
8. M. S. Wolfe. *Nat Rev Drug Discov 1*, 859-866 (2002).
9. J. T. Coyle, D. L. Price, M. R. DeLong. *Science 219*, 1184-1190 (1983).
10. Y. Hashimoto, Y. Ito, T. Niikura, Z. Shao, M. Hata, F. Oyama, and I. Nishimoto. *Biochem Biophys Res Commun 283*, 460-468 (2001).
11. Y. Hashimoto, T. Niikura, Y. Ito, H. Sudo, M. Hata, and E. Arakawa. *J Neurosci 21*, 9235-9245 (2001).
12. Y. Hashimoto, T. Niikura, H. Tajima, T. Yasukawa, H. Sudo, Y. Ito, Y. Kita, M. Kawasumi, K. Kouyama, M. Doyu, G. Sobue, T. Koide, S. Tsuji, J. Lang, K. Kurokawa, and I. Nishimoto. *Proc Natl Acad Sci USA 98*, 6336-6341 (2001).
13. P. Vito, B. Wolozin, J. K. Ganjei, K. Iwasaki, E. Lacana, and L. D'Adamio. *J Biol Chem 271*, 31025-31028 (1996).
14. B. Martoglio and B. Dobberstein. *Trends Cell Biol 8*, 410-415 (1998).
15. G. Von Heijne. *J Membr Biol 115*, 195-201 (1990).
16. Y. Hashimoto, H. Suzuki, S. Aiso, T. Niikura, I. Nishimoto, and M. Matsuoka. *Life Sci 77*, 3092-3104 (2005).
17. Y. Hashimoto, O. Tsuji, T. Niikura, Y. Yamagishi, M. Ishizaka, M. Kawasumi, T. Chiba, K. Kanekura, M. Yamada, E. Tsukamoto, K. Kouyama, K. Terashita, S. Aiso, A. Lin, and I. Nishimoto. *J Neurochem 84*, 864-877 (2003).
18. D. Benaki, C. Zikos, A. Evangelou, E. Livaniou, M. Vlassi, E. Mikros, and M. Pelecanou. *Biochem Biophys Res Commun 329*, 152-160 (2005).
19. H. J. Dyson, M. Rance, R. A. Houghten, P. E. Wright, and R. A. Lerner, II. *J Mol Biol 201*, 201-217 (1988).
20. S. R. Lehrman, J. L. Tuls, and M. Lund. *Biochemistry 29*, 5590-5596 (1990).
21. T. Niikura, Y. Hashimoto, H. Tajima, and I. Nishimoto. *J Neurosci Res 70*, 380-391 (2002).
22. H. J. C. Berendsen, D. J. van der Spoel, and R. van Drunen. *Comp Phys Comm 91*, 43-56 (1995).
23. E. Lindahl, B. Hess, and D. J. van der Spoel. *Mol Mod 7*, 306-317 (2001).
24. W. F. Van Gunsteren, S. R. Billeter, A. A. Eising, P. H. Hünenberger, P. Krüger, A. E. Mark, W. R. P. Scott, and I. G. Tironi. (Hochschulverlag AG an der ETH Zürich, Zürich 1996).
25. D. Van der Spoel, A. R., van Buuren, E. Apol, P. J. Meulenhoff, D. P. Tieleman, A. L. T. M. Sijbers, B. Hess, K. A. Feenstra, E. Lindahl, R. van Drunen, and H. J. C. Berendsen. Department of Biophysical Chemistry, (University of Groningen, Groningen, The Netherlands, 2002).
26. H. J. C. Berendsen, J. P. M. Postma, W. F. van Gunsteren, A. Di Nola, and J. R. J. Haak. *Chem Phys 81*, 3684-3690 (1984).
27. B. Hess, H. Bekker, H. J. C. Berendsen, and J. G. E. M. Fraaije. *J Comp Chem 18*, 1463-1472 (1997).
28. T. Darden, D. York, and L. J. Pedersen. *Chem Phys 98*, 1463-1472 (1993).
29. W. Kabsch and C. Sander. *Biopolymers 33*, 2577-2637 (1993).
30. R. Aurora, T. P. Creamer, R. Srinivasan, and G. D. Rose. *J Biol Chem 272*, 1413-1416 (1997).
31. M. Buck and Q. ReV. *Biophys 31*, 297-355 (1998).
32. R. Chitra and P. E. Smith. *J Phys Chem B 105*, 11513-11522 (2001).

Date Received: February 4, 2008

Communicated by the Editor Manju Bansal